High-accuracy low-cost generalized complex pruned Volterra models for nonlinear calibration

Cristian Bocciarelli, Francesco Centurelli, *Senior Member, IEEE*, Pietro Monsurrò, Giuseppe Scotti, *Senior Member, IEEE,* Valerio Spinogatti, Pasquale Tommasino, and Alessandro Trifiletti

***Abstract*—Nonlinear calibration allows enhancing the performance of analog and radiofrequency circuits by digitally correcting nonlinearities. Often, calibration is performed in the complex baseband domain, and Volterra models are used. These models have hundreds of coefficients, and easily become computationally unfeasible. This is worse in complex Volterra models, because high-order Volterra terms require summing multiple products of the input signal. We propose a generalized complex Volterra model based on one relaxation of Volterra theory: all the nonlinear monomial terms in the model are considered separately, even if they correspond to a single real coefficient in complex Volterra theory. This produces more accurate models, though with a larger number of coefficients. We thus extensively prune the model by means of OMP and OBS techniques. The resulting models have fewer coefficients and/or better accuracy than conventional Volterra models, resulting in a significantly improved accuracy-complexity trade-off. These results are validated in the experimental calibration of a commercial IF amplifier. The resulting model achieves the same accuracy, with 9 free parameters and 34 multiplications, as the standard Volterra model with 12 parameters and 266 multiplications, resulting in a 25% reduction in the number of parameters, and an 87% reduction in the number of multipliers.**

***Index Terms*—Digital calibration, nonlinear models, complexity reduction, amplifiers, analog circuits, optimal brain surgeon, orthogonal matching pursuit.**

I. Introduction

MODERN electronic systems heavily rely on digital signal processing. The digital conversion of the signal allows calibration in the digital domain, enabling the so called *digitally-assisted analog electronics*, where digital algorithms improve the performance of analog blocks [1-2]. Power amplifiers [3-6], IQ mixers [7-8] and ADCs [9-13] can be digitally enhanced. Calibration can correct linear errors, as in time-interleaved (TI) ADCs [14-16], but can also be exploited to reduce the nonlinearity of system components [12], and of the system as a whole [11-13].

Volterra models are often used to describe weakly nonlinear continuous systems where memory effects have to be taken into account [17]. However, depending on their maximum order of nonlinearity and memory depth, these models often require a huge number of parameters, resulting in high computational complexity and estimation problems.

These issues are particularly significant for Volterra models in the complex domain [18], because these models have much higher computational cost, as each high-order Volterra coefficient multiplies the sum of multiple delayed, phase shifted and eventually frequency modulated product terms, which need to be computed in real time. Hence, setting up a complex Volterra model is computationally expensive. Furthermore, the theory is restrictive, yielding models that are not very accurate despite the huge resource cost.

In this paper we propose a generalized class of complex Volterra models based on the removal of one key assumption: each monomial term in high-order Volterra kernels is assumed to be independent from the others, with a separate coefficient. The removal of this hypothesis yields a class of models which is more accurate than conventional complex Volterra models, at the cost of a significantly larger number of coefficients.

Hence, computational costs are increased and estimation is more cumbersome. To compensate for this problem, pruning is used to reduce the computational complexity of the generalized complex Volterra models, yielding much more compact models with comparable linearity. Pruning is performed using a combination of the Orthogonal Matching Pursuit (OMP) [18-20] and Optimal Brain Surgeon (OBS) [18, 21-22] techniques.

The resulting pruned model can be either more accurate or simpler than the original model after pruning, and much easier to set up: in fact, a pruned Volterra model would require the computation of many polynomial basis functions, including phase shifts and frequency modulations, whereas generalized Volterra models only use monomials. Hence, the proposed model is more general, and thus more accurate, but also more flexible, and thus more easily pruned to a computational cost which is much lower than that of conventional complex Volterra models. It is thus possible to improve the accuracy-complexity trade-off to obtain nonlinear models that are at the same time more accurate, computationally simpler, and easier and faster to estimate, owing to a lower number of nonlinear coefficients.

This important result is verified experimentally in the calibration of an IF amplifier: a 25% reduction in the number of free parameters to estimate, and an 87% reduction in the number of complex multipliers required to correct the output, is achieved with respect to the conventional complex Volterra model.

The contributions of this paper can thus be summarized as follows:

- We propose a novel class of complex Volterra models which improves the accuracy-complexity trade-off. The new class of models is obtained by removing a

[1]Authors are with the Department of Information, Electronics and Telecommunication Engineering, Sapienza University of Rome, Rome, Italy (e-mail: pietro.monsurro@uniroma1.it).

hypothesis from conventional complex Volterra theory and is therefore a generalization of the latter.

- The new class of models is validated experimentally for the calibration of an IF amplifier. A performance comparison between the generalized and the conventional Volterra model is carried out, before and after pruning.

It should be remarked that the generalized class of models includes Volterra models as a special case, and thus cannot be less accurate than Volterra models: it is in fact more accurate, as experimentally shown in this paper. The problem of the increased number of free coefficients can be effectively solved by extensive pruning, with experimental evidence that the generalized models are more accurate for the same number of free coefficients. The main reason for the significantly reduced computational complexity is that a single term of order P in conventional Volterra theory requires the sum of 2^{P-1} monomials of order P, whereas in the generalized model only one monomial needs to be computed.

The paper is organized as follows. Section II summarizes Volterra models in the real and complex domains. Section III proposes a new generalized Volterra model, and summarizes the pruning technique employed to reduce its complexity. Section IV describes the experimental setup and discusses the experimental results. Section V concludes.

II. Volterra Models in the Real and Complex Domains

Nonlinear calibration techniques attempt to correct linear and nonlinear errors arising in electronic systems owing to active devices. There is no standard model for nonlinearities, especially for dynamic nonlinearities, i.e., nonlinear effects with memory: Volterra series are often used, but these models easily become unmanageable owing to the large number of coefficients.

In this paper we define a subclass of linear-in-the-parameters (LIP) feedforward models, a class of models which also includes feedforward Volterra models, FIR filters, polynomial nonlinear models, but also functional link artificial neural networks (FLANN) models with linear output layers [23], Hammerstein models [24], and others. Since they are linear in the parameter space, such models allow using linear estimation techniques, which are convex, numerically simple, and well-posed [25].

As we assume the system is sampled, we model the block under calibration as a discrete-time system. The input signal is $x[n]$, sampled at a rate f_S, and produced by a DAC whose linearity and noise are assumed to be better than that of the amplifier under calibration. The output of the device to be calibrated is $y[n]$, which is sampled, at the same rate, by an ADC, whose accuracy is also supposed to be better than that of the device to be calibrated. The input is considered to be an IF signal of bandwidth B_W around the carrier f_C, with $0 < f_C - \frac{B_W}{2} < f_C + \frac{B_W}{2} < \frac{f_S}{2}$.

In general, the nonlinear function describing the device will not be known, but it will be nonlinear and with memory, so that the output of the system is a nonlinear function of the present and past values of the input. Of course, noise shall also be considered.

Digital calibration consists in approximating the inverse function of the system in the digital domain, so that the calibrated output $z[n]$ will be as close as possible to the (known) input $x[n]$. In this way, the deterministic errors affecting $y[n]$ will ideally be removed, if the system is invertible:

$$z[n] = g(y[n], \dots, y[n-M]) \approx x[n] \tag{1}$$

Since such a model is unworkable, we focus on models which are linear-in-the-parameters and feedforward:

$$z[n] = \sum_0^{L-1} \beta_l g_l\big[y[n], \dots, y[n-M]\big] \tag{2}$$

This model has L unknown parameters, β_l, which are the coefficients of the linear combination of the known linear and nonlinear functions $g_l(\cdot)$ of the input signal, including its past values, up to a delay M. The use of LIP models ensures that a wide array of estimation algorithms for linear models can be employed: batch least squares, recursive least squares (RLS), least mean squares (LMS) [25], etc. In fact, linear estimation techniques, which are well known, numerically efficient and stable, and globally optimal, can be used to estimate any LIP model.

Another assumption implicit in (2) is that the output only depends on the input, i.e., it does not depend on the past values of the output. Such models are called feedforward, as there is no feedback of the output toward the input, and are a generalization of finite impulse response (FIR) linear filters. For instance, if $g_l\big[y[n], \dots, y[n-M]\big] \equiv y[n-l]$, and $L = M + 1$, the model in (2) becomes a FIR filter, which is the workhorse of linear equalization techniques in telecommunications. On the other hand, if $g_l\big[y[n], \dots, y[n-M]\big] \equiv y^l[n]$, the model in (2) becomes a standard polynomial model with static nonlinearities. Volterra models are an example of LIP feedforward models.

A. Real Volterra models

The Volterra model is the sum of kernels of degree $p = 1, \dots, P$, where monomials of order p are obtained from the input $y[n]$ using lagged terms up to a delay $M(p)$, where the memory length can be a function of the degree, to minimize model complexity. Since products are commutative, delays can be put in non-decreasing order. Hence, we focus on non-decreasing tuples, and write the output of the kernel of degree p as:

$$z^p[n] = \sum_{i_1=0}^{M_p} \cdots \sum_{i_p=i_{p-1}}^{M_p} \beta_{i_1 \dots i_p} y[n-i_1] \cdots y\big[n-i_p\big] \tag{3}$$

Finally, the output of the Volterra model is the sum of the outputs of the Volterra kernels, up to the highest order P:

$$z[n] = \sum_{p=1}^{P} z^p[n] \tag{4}$$

The model may include a term of order 0, which represents the dc offset.

The main problem with Volterra models is the number of coefficients: a 5th-order model with $M = 4$ would have 126 free parameters. The computational cost of Volterra models depends on the number of free parameters which need to be estimated, plus a setup cost to compute all the monomials in the Volterra kernels. The number of free parameters to estimate has a direct impact on the complexity of the estimation technique, on estimation convergence time, and on the stability of estimation algorithms. Hence, model pruning is of the essence to reduce model complexity and improve numerical stability and convergence time, i.e., the number of known samples required to identify the system.

Furthermore, real-time correction, even with fixed (already identified) parameters, requires a fixed cost per sample, comprising the computation of the basis functions which form the Volterra kernels and the calculation of the linear combinations of basis functions which allow computing the corrected output, as in Eq. 2.

B. Complex Volterra models

Usually, equalization in communication systems is performed in the complex domain [26], after demodulation and carrier and timing recovery. The goal is to minimize the linear and nonlinear Inter-Symbol Interference (ISI) and allow symbol decision with the lowest Error Vector Magnitude (EVM) and Symbol Error Rate (SER). Hence, we define the intermediate frequency (IF) and baseband frequency (BF) signals, where ω_0 is the normalized carrier frequency $\omega_0 = 2\pi f_C T_S$, with f_C the carrier frequency in Hz, and T_S the sampling period:

$$y_{IF}[n] = \Re\{y_{BF}[n]e^{j\omega_0 n}\} \tag{5}$$

A FIR filter can be written in the IF domain as:

$$z_{IF}[n] = \sum_{l=0}^{L-1} h_l y_{IF}[n-l] = \Re\left\{\sum_{l=0}^{L-1} h_l y_{BF}[n-l]e^{j\omega_0(n-l)}\right\} \tag{6}$$

If we rewrite the second expression, we obtain:

$$z_{BF}[n] = \sum_{l=0}^{L-1} h_l y_{BF}[n-l]e^{-j\omega_0 l} \tag{7}$$

Hence, a linear filter in the IF domain is equivalent to a linear filter in the BF domain, with the same (real) coefficients h_l, if the BF samples are phase rotated by $e^{-j\omega_0 l}$ and delayed by l.

Similar calculations hold for Volterra kernels of higher degrees. For instance, a generic quadratic term can be written as:

$$x_{IF}[n-l]x_{IF}[n-m] = \\ = \Re\{x_{BF}[n-l]e^{j\omega_0(n-l)}\}\Re\{x_{BF}[n-m]e^{j\omega_0(n-m)}\} \tag{8}$$

Using the identity $\Re\{x\} = \frac{1}{2}(x + x^*)$, we get Eq. (9) reported at the bottom of the page.

Hence, a second-order kernel is the sum of two second-order monomials, one frequency modulated by $e^{j\omega_0 n}$, the other by $e^{-j\omega_0 n}$, which correspond to the terms around $2f_C$ and dc, respectively.

Similar relations can be obtained for higher-order kernels. Hence, IF kernels can be expressed in terms of the BF components, and the Volterra coefficients remain real and have the same value. The higher-order terms can be modulated around frequencies 0, ω_0 or multiples.

From the above equations we notice several important aspects. First, the complex Volterra kernel has the same number of (real) parameters than the real Volterra kernel, with the same coefficient values, because they are equivalent models. But complex Volterra kernels of the second-order require the sum of two complex products (9) to compute the basis functions, and these products also require phase shifting and frequency translation. This is even worse in higher-order kernels: third-order kernels require the sum of four terms, and fifth-order terms the sum of sixteen terms: the product of P terms such as $\Re\{x\} = \frac{1}{2}(x + x^*)$ creates 2^P products, which are paired into 2^{P-1} terms when the final real value is computed. Hence, complex Volterra models are more expensive to set up, requiring more operations to compute all the basis functions.

Some of these terms are modulated around carriers different from f_C and may be removed in narrowband systems, but in general this is not possible in wideband systems.

These issues are solved in the next Section, where generalized Volterra kernels are defined, which are more general, and thus more accurate, and can be pruned to smaller models, and thus are less expensive in terms of resources (after pruning). Their higher accuracy is due to their higher generality, whereas the lower computational cost depends on two factors: first, the setup cost is significantly reduced because each parameter of the model is only multiplied by a monomial, instead of the sum of 2^{P-1} monomials; second, the number of coefficients which remain after pruning is lower, for the same accuracy.

III. Generalized Volterra models

Complex Volterra models are equivalent to real Volterra models but operate on the baseband complex components instead of the intermediate frequency signal.

There is one hypothesis behind the derivation of complex Volterra model: all the monomials of the basis functions are multiplied by the same parameter. To keep the explanation simple, we consider a third-order Volterra model with no delays:

.

$$x_{IF}[n-l]x_{IF}[n-m] = \frac{1}{2}\Re\{x_{BF}[n-l]x_{BF}[n-m]e^{j\omega_0(2n-l-m)} + x_{BF}[n-l]x_{BF}^*[n-m]e^{j\omega_0(-l+m)}\} = \\ = \tfrac{1}{2}\Re\{(x_{BF}[n-l]x_{BF}[n-m]e^{j\omega_0(n-l-m)} + x_{BF}[n-l]x_{BF}^*[n-m]e^{j\omega_0(-n-l+m)})e^{j\omega_0 n}\} \tag{9}$$

$$z_{BF}[n] = \sum_{p=1}^{3} z_{BF}^{p}[n] \quad (10a)$$
$$z_{BF}^{1}[n] = \beta_{0}^{1} y[n] \quad (10b)$$
$$z_{BF}^{2}[n] = \frac{1}{2}\beta_{00}^{2}(y^{2}[n]e^{j\omega_0 n} + |y[n]|^{2}e^{-j\omega_0 n}) \quad (10c)$$
$$z_{BF}^{3}[n] = \frac{1}{4}\beta_{000}^{3}(y^{3}[n]e^{j2\omega_0 n} + 3|y[n]|^{2}y[n]) \quad (10d)$$

Three of the four terms in the third-order kernel are equivalent for 0 lags, but are in general different. Also, all phase shifts are 0 for 0 lags, but in general will not be so. This simple model has 1 first-order term, 2 second-order terms and 2 third-order terms (instead of 4), plus three frequency modulators. The model has only three unknowns, $\beta_{\{0\}}^{p}$, because $M(p = \{1,2,3\}) = 0$. Of course, such model would be much more complex for larger delays and orders.

The hypothesis in complex Volterra theory is that the polynomial terms for the same kernel and lag shall be multiplied by the same coefficient. By removing this hypothesis we obtain a new generalized model, that has $2^{p-1} - 1$ more free coefficients for each term of degree p. In our toy example (Eq. 10), there would be 1 additional term for the 2nd-order kernel, and 3 for the third-order kernel (actually, for zero lags two such terms are identical).

This relaxation will yield a more complex model with better accuracy, because it has more degrees of freedom: the original model can be obtained by constraining the related coefficients to be equal. The fact that the obtained model is more general implies that it will be more accurate, if there are no estimation problems due to the larger number of free parameters. Such an issue will be tackled through pruning in the next sub-section. In the same simplified assumptions seen above, the proposed model will be:

$$z_{BF}[n] = \sum_{p=1}^{3} z_{BF}^{i}[n] \quad (11a)$$
$$z_{BF}^{1}[n] = \beta_{0}^{1} y[n] \quad (11b)$$
$$z_{BF}^{2}[n] = \beta_{00a}^{2} y^{2}[n]e^{j\omega_0 n} + \beta_{00b}^{2}|y[n]|^{2}e^{-j\omega_0 n} \quad (11c)$$
$$z_{BF}^{3}[n] = \beta_{000a}^{3} y^{3}[n]e^{j2\omega_0 n} + \beta_{000b}^{3}|y[n]|^{2}y[n] \quad (11d)$$

There are now five unknown terms instead of three. The original model can be obtained if $\beta_{000a}^{3} = \frac{1}{3}\beta_{000b}^{3} = \frac{1}{4}\beta_{000}^{3}$ and $\beta_{00a}^{2} = \beta_{00b}^{2} = \frac{1}{2}\beta_{00}^{2}$.

The generalized model will have a much larger number of free parameters. Because of the large increase in model coefficients, pruning is required to reduce model complexity.

A. Pruning via OMP and OBS

Though pruning of the model is of the essence to reduce model complexity, there is another approach that is widely exploited in the literature for the same reason: restricting the Volterra models with a priori hypotheses on the structure of the nonlinear kernels.

For instance, forcing $M_P = 0$ will yield a model with static nonlinearities, which is the simplest (though usually inaccurate) nonlinear model which can be used: the number of nonlinear coefficients would be $P - 1$, one for the 2nd-order term, one for the 3rd-order term, and one for each order up to P. A static nonlinear model is a subset of Volterra models, but based on very restrictive hypotheses on the nature of nonlinearities.

A less restrictive class of models are memory polynomial (MP) models [27], which force distortions terms to have the same delay, so that $i_1 = i_2 = \cdots = i_p$ for each kernel of order p, with $i_1 = 0, \ldots, M_p$. Hence, there would be M_p terms of order p, instead of a number of terms which grows as $M_p^p/p!$ as in Volterra kernels. Also these models are included in Volterra theory, though they represent a small subset of Volterra models, given the strong restrictions on the delay indexes.

Generalized memory [28] polynomials are even less restrictive because they allow products with the leading and lagging terms of the samples.

Other models lift the hypothesis of linear dependence of the parameters and are thus not LIP, such as modified generalized memory polynomials (MGMP) [27], and are not considered in this paper.

Pruning uses a different approach: the choice of the parameters to consider is not made a priori, as in restricted Volterra models, but results from some algorithm which chooses the most promising subset of parameters from the data.

The desired response of the system, $x[n]$, can be recorded in a column vector V of size $N \times 1$. The L linear and nonlinear functions of the system output $y[n]$, which correspond to the monomials of the Volterra kernels, can be put in a design matrix X of size $N \times L$, and the unknown parameters β are a column vector of size $L \times 1$. Hence:

$$V = X\beta \leftrightarrow e = V - X\beta \quad (12)$$

Model estimation consists in minimizing the energy of the error vector e, choosing the parameter vector β optimally. Such an estimation problem can be performed using conventional least squares techniques, under the assumption that the model is well specified: $N \gg L$, and the columns of X are not linearly dependent. If these hypotheses fail, β cannot be robustly estimated.

Orthogonal Matching Pursuit (OMP) is the standard technique for model pruning from the simplest to the most complex model: the algorithm is greedy, and thus suboptimal, and iterative, choosing one additional input vector per iteration [19-20]. The OMP algorithm computes the correlations between the desired output V and the columns of X, and selects the column with the highest correlation: this provides the optimal model of size 1, i.e., the model with only one parameter which minimizes the error energy. Once a first parameter is obtained, the selected column is used to regress both the desired output and all the remaining columns of X. This regression makes both V and X orthogonal to the selected variable (the new X will have $L - 1$ columns). The algorithm can be reiterated $L_{omp} \leq L$ times, and selects a model with one additional parameter at each iteration. There is no guarantee that the algorithm will select the optimal model with L_{omp} parameters, because the algorithm is greedy and optimal only for one step. However, OMP is robust, easy to use, and usually effective. Moreover, there is no computationally feasible alternative,

because there are $\frac{(L+L_{omp})!}{L!L_{omp}!}$ possible subsets of L_{omp} columns of the L columns of X, and it is unfeasible to try all the combinations, though a brute force method would yield the optimal model by exhaustive search.

On the other hand, the Optimal Brain Surgeon (OBS) algorithm [18, 21-22] starts from the full model and removes one variable at the time, selecting the one that influences the residual error the less. The impact of each variable on the error depends on the curvature of the error curve and the value of the parameter, and variables which are either small or have small curvature are removed first. The goal is to reiterate the algorithm many times, to obtain a model of complexity $L_{obs} \ll L$ while retaining accuracy.

The two techniques operate in opposite directions: the OMP from the simplest to the most complex model, and the OBS from the complete to the simplest model. The best technique is the one that selects the minimum-error pruned model for a given complexity: in general, none of the two techniques outperforms the other for all desired pruning levels, and combining the two allows finding a better approximation of the complexity-accuracy trade-off [18].

To the extent that $L_{omp}, L_{obs} \ll L$, and that the pruned model is not much less accurate than the full model, the new pruned model will have much lower computational cost, lower estimation time, and better numerical stability and accuracy properties. Since heavily correlated columns are never selected, the resulting pruned models are usually well behaved: if a column were linearly dependent on the previously chosen ones, its residual would be zero, and it would be discarded.

B. Estimating complex models

Estimation in the complex domain always yields complex desired vectors V and design matrices X, but in the conventional Volterra model the unknown parameters β remain real. We use the subscripts R and I for the real and imaginary parts of the vectors, respectively. The error is $e = y - X\beta = = (y_R - X_R\beta) + j(y_I - X_I\beta)$. The Euclidean norm of the error is $e^T e = e_R^T e_R + e_I^T e_I$, where the superscript T is the transpose operator: minimizing the error implies minimizing the sum of the error on the real and imaginary terms. Hence, the optimal Euclidean norm model is:

$$\beta = \left(\begin{pmatrix} X_R^T & X_I^T \end{pmatrix} \begin{pmatrix} X_R \\ X_I \end{pmatrix} \right)^{-1} \left(\begin{pmatrix} X_R^T & X_I^T \end{pmatrix} \begin{pmatrix} V_R \\ V_I \end{pmatrix} \right) \tag{13}$$

Hence, complex models with real coefficients can be estimated as real models with real coefficients. In the case of Equation (13) the real equivalent model has L unknowns and $2N$ equations.

IV. Experimental Results and Discussion

This Section describes the experimental setup and discusses the results. A commercial IF amplifier has been measured with QAM-64 input waveforms, and calibrated with and without pruning, using both the conventional and the proposed generalized Volterra models.

A. Experimental setup

The ZX60-100VH+ amplifier [27] has been tested. The setup includes 3dB of attenuation before the amplifier, and 30dB of attenuation [28] after the amplifier. The nominal gain of the amplifier is 36dB, hence the overall chain has an expected gain of about 3dB. The full-scale value of the DAC is 1Vpp and the input waveform has a peak-to-peak swing of 900mVpp. The full-scale value of the ADC is 2Vpp, so that the expected output swing of the received waveform is about 32% of the full swing of the ADC. The amplifier is driven close to the back-off input power, to make distortions evident.

The experimental setup is composed of an FPGA board connected to an ADC-DAC FMC150 board [29]. The board has two 250MS/s 14-bit ADCs and two 500MS/s 16-bit DACs. Only one DAC and ADC are used, and both are clocked synchronously at 250MS/s. A file containing 16.384 samples is sent to the FPGA and then to the DAC, whereas the ADC records 131.072 samples, i.e., 8 copies of the same input (the DAC repeats the same waveform continuously). Several QAM-64 waveforms have been acquired to allow averaging and investigate noise performance.

The DAC includes a built-in 82MHz filter, and both the ADC and the DAC are AC-coupled, with a low cut-off frequency of 3 and 0.4MHz, so that the effective bandwidth of the system is about 3-80MHz. The measurement chain includes an anti-aliasing lowpass SLP-100 filter by Mini Circuits, with 100MHz bandwidth [30]. The DAC-ADC chain, including both filters, has an EVM of less than 0.4%, an order of magnitude lower than those of the amplifier under calibration, so that the error – nonlinear and stochastic – due to the setup is negligible.

B. Characterization of the IF amplifier

Figure 1 shows the transmitted and received signal spectra. The input has 50MHz bandwidth around a 50MHz carrier frequency, and spectral regrowth is clearly evident in the output spectrum (red) with respect to the input spectrum (black).

The output spectrum has about 3dB gain loss at 80MHz, compatibly with the 80MHz pulse-shaping lowpass filter after the DAC. The nonlinear spectral regrowth after the amplifier is attenuated after 100MHz by the anti-aliasing lowpass filter before the ADC.

Figures 2 and 3 show the EVM, SER and constellation after equalization with 9 coefficients. A linear model with 9 coefficients only corrects linear errors, and it is evident that equalization alone is not enough for reliable reception of the QAM-64 waveforms. Longer filters do not reduce the EVM, because most errors are nonlinear, and the frequency response of the setup is rather flat over the 50MHz bandwidth.

The residual error is not due to noise, because a total of 14 waveforms have been acquired and averaged (with a theoretical process gain of 11.5dB), but no difference between the averaged and non-averaged EVM have been observed. Hence, most of the EVM is due to residual nonlinear ISI, and not to noise, otherwise the EVM would have fallen with averaging.

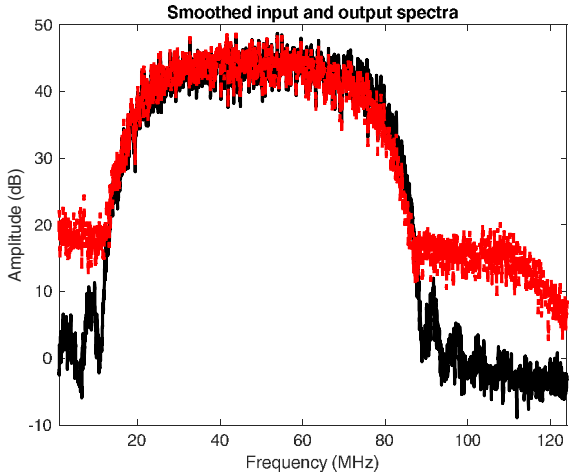

Fig. 1. Input (black) and output (red) spectrum. Spectral regrowth is clearly visible at the output. Attenuation after 100MHz is due to the antialiasing filter.

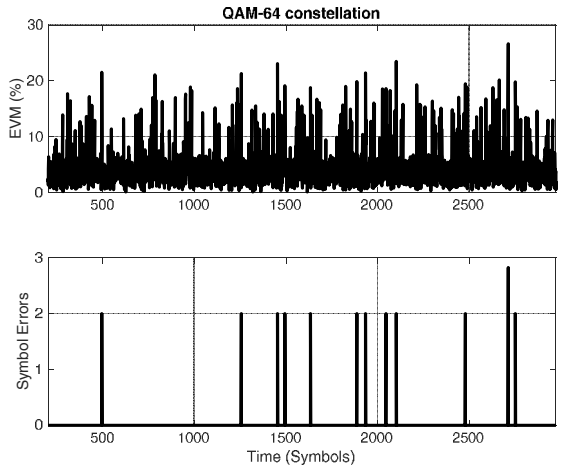

Fig. 2. EVM (top) and SER (bottom) after equalization with 9 linear coefficients and offset correction. Transmission errors are evident, and the EVM is too large. Longer linear filters do not improve accuracy.

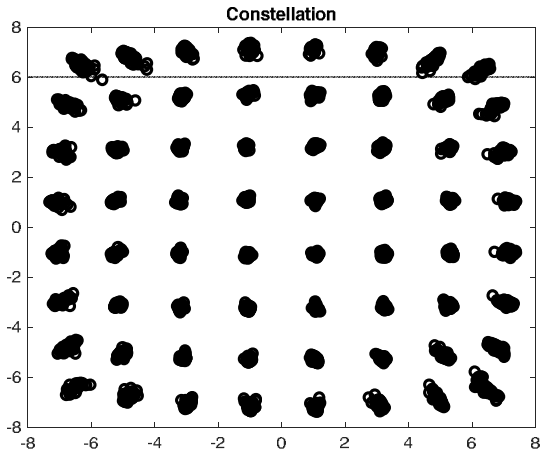

Fig. 3. Received constellation after equalization. The QAM-64 constellation should form a square of 8 dots per dimension. Noise is limited (the central dots are small), but heavy distortion occurs at the corners, owing to nonlinear effects. Such distortions produce transmission errors, as evidenced in Fig. 2.

Hence, nonlinear models are required to improve EVM and SER, as the residual error is neither stochastic nor linear.

C. Calibration with the conventional Volterra model

Figures 4 and 5 show the SER, EVM and constellation after calibration with a conventional Volterra model with lag structure (8, 4, 4, 2, 2). This means that the linear section has a maximum delay of 8, the quadratic and cubic parts a maximum delay of 4, and the 4th- and 5th-order sections a maximum delay of 2. The model has 96 coefficients and needs pruning to reduce its computational cost, but EVM falls to 2.8% and SER to 0.

Figure 6 shows the pruning of the conventional Volterra model using the OMP and OBS methods. Figure 7 shows the constellation after pruning to 22 coefficients. EVM is 3.1% and no transmission errors are present.

D. Calibration with the generalized Volterra model

Figures 8 and 9 show the impact of calibration with the generalized Volterra model. The lag structure of the 5th-order

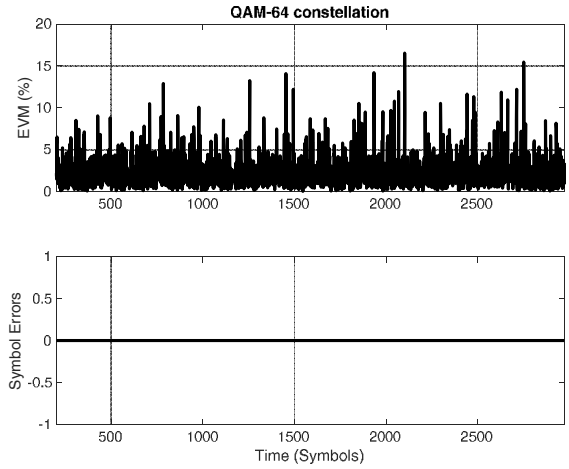

Fig. 4. EVM (top) and SER (bottom) after calibration with the conventional Volterra model. No transmission errors are present, and EVM is 2.8%.

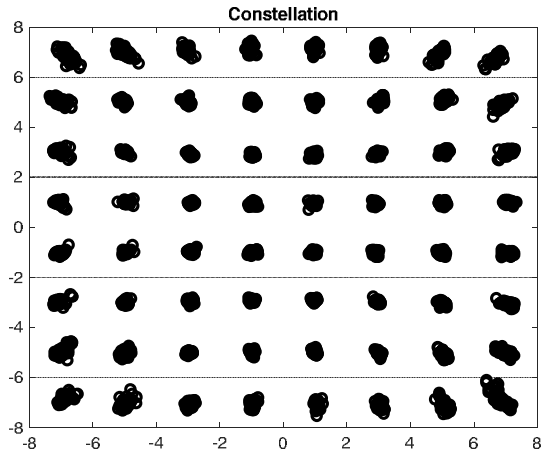

Fig. 5. Received constellation after calibration with the conventional Volterra model. The QAM-64 constellation should form a square of 8 dots per dimension. Noise is limited (the central dots are small), and distortion is still evident at the corners, but overall the symbols are well spaced.

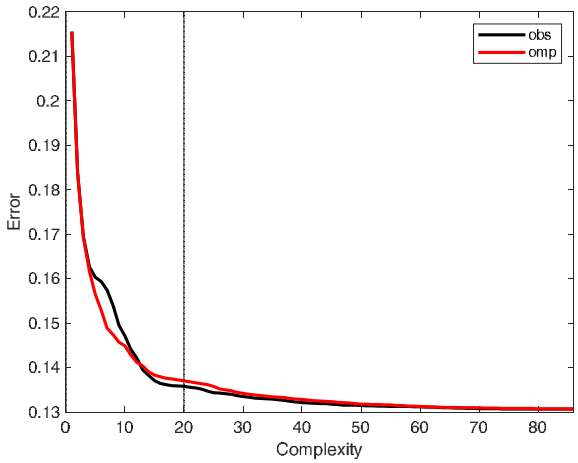

Fig. 6. Pruning of the conventional Volterra model using the OMP and OBS methods.

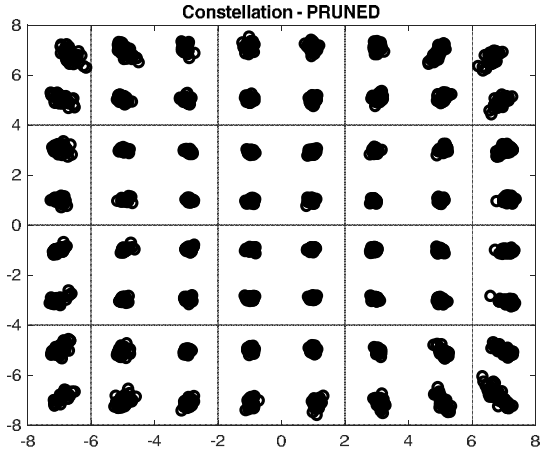

Fig. 7. Received constellation after calibration with the conventional Volterra model after pruning to 22 coefficients, 10 linear and 12 nonlinear.

model is (8, 4, 4, 2, 2), so that there are 9 linear coefficients, but many more nonlinear ones. The total number of coefficients before pruning is 636, making the model completely impractical. The resulting error is 2%, significantly lower than in the conventional Volterra model (Fig. 6), but at a much larger computational cost. The constellation in Fig. 9 is much better spaced and closer to the ideal square of 8 symbols per dimension than with the conventional Volterra model (Fig. 7), implying that the model is significantly more accurate. Pruning is of the essence, however, to make it practical.

Figure 10 shows the effect of pruning with the OMP and OBS methods, while Fig. 11 shows the constellation after pruning to 18 coefficients, 10 for the linear part and 8 for the nonlinear part. EVM is 3.1% and SER is 0, though the constellation is again distorted.

Pruning to 9 nonlinear coefficients of the generalized Volterra model yields the same EVM as pruning to 12 of the conventional Volterra model. Furthermore, the basis functions of the generalized Volterra model are cheaper to compute,

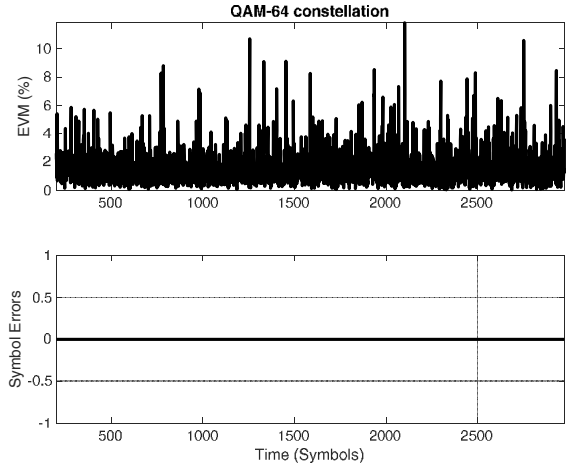

Fig. 8. EVM (top) and SER (bottom) after calibration with the generalized Volterra Model with 636 coefficients. No transmission errors are present, and EVM is 2.0%. However, the model is expensive and impractical.

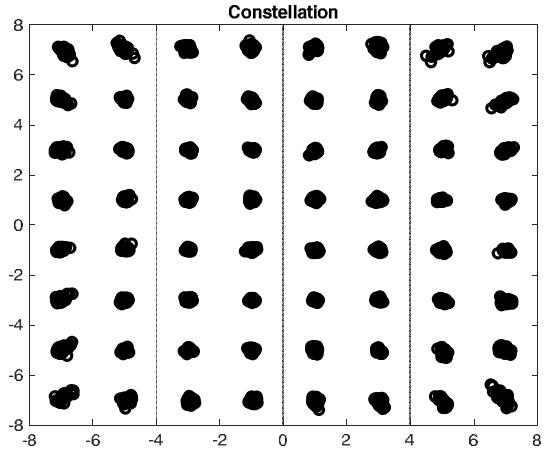

Fig. 9. Received constellation after calibration with the generalized Volterra model. The QAM-64 constellation should form a square of 8 dots per dimension. Noise is limited (the central dots are small), and some distortion is still evident at the corners, but overall the symbols are well spaced. Unfortunately, the model has 636 coefficients and is impractical without pruning.

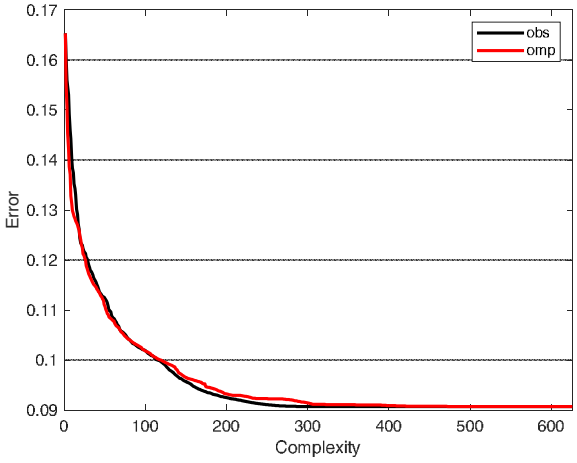

Fig. 10. Pruning of the generalized Volterra model.

because they are just monomials, and not the sum of 2^{p-1} monomial terms for the conventional Volterra kernel of order p. Hence, there is a great advantage in terms of computational complexity, and also an advantage in terms of estimation time and numerical stability, as both depend on the number of the parameters to estimate.

Figures 12 and 13 compare the results of pruning of the two models. The conventional Volterra model starts with 96 coefficients, while the generalized Volterra model with 636. However, pruning is much more effective in the generalized Volterra model, resulting in a more accurate and cheaper model after extensive pruning. The two figures differ because Fig. 12 considers complexity as the number of coefficients to estimate, whereas Fig. 13 reports the setup cost required to compute all the basis functions, as the number of complex products required to compute each of them. The setup cost in Fig. 13 is paid for each calibrated output (once per sample), whereas the number of coefficients in Fig. 12 influences the cost of the estimation algorithm to compute the optimal model coefficients.

After pruning to 9 nonlinear coefficients (and 10 linear coefficients), only 1 of the 2nd-order term remains, plus 6 3rd-order terms, and 2 5th-order terms. Hence, the setup cost consists in computing 9 monomial terms, most of them of the 3rd-order.

Compared with the conventional model, which achieves the same EVM and SER with 12 coefficients, 4 of the 2nd-order, 6 of the 3rd-order, and 2 of the 5th-order, the setup cost is much lower, because there are 9 monomials to be computed, instead of 64 (2^{p-1} for each p-order term).

Hence, not only 9 coefficients instead of 12 are to be estimated, but 9 monomial terms (of various orders) instead of 64 are to be computed for each sample to perform the real-time computation of the calibrated output.

Considering that the computation of each monomial of order p requires p complex multiplications ($p-1$ for the lagged input terms, and one for the phase shifter), plus eventually another complex multiplication for the terms that are frequency modulated, the setup cost of the conventional model pruned to 12 coefficients is 266 complex multiplications. On the other hand, the setup cost of the generalized model with 9 coefficients is only 34 complex multiplications: an 87% reduction in setup cost is thus obtained.

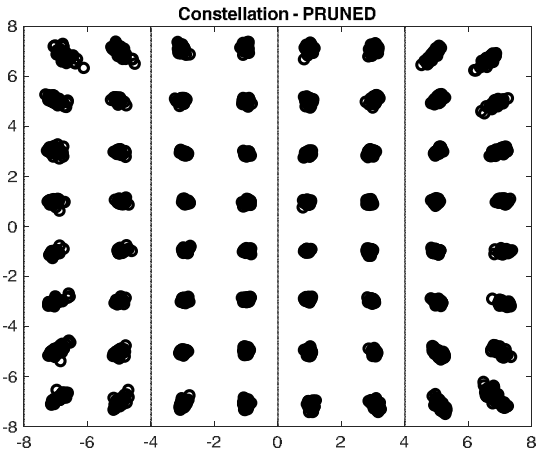

Fig. 11. Constellation after pruning to 19 coefficients (10 linear and 9 nonlinear).

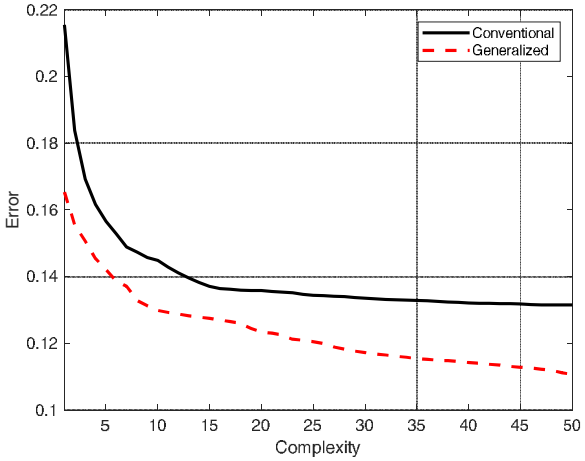

Fig. 12. Comparison of pruning for the two models in terms of number of coefficients: conventional (black) and generalized (red) models. The generalized model is much more accurate for the same number of coefficients, yielding a significantly smaller model for the same accuracy.

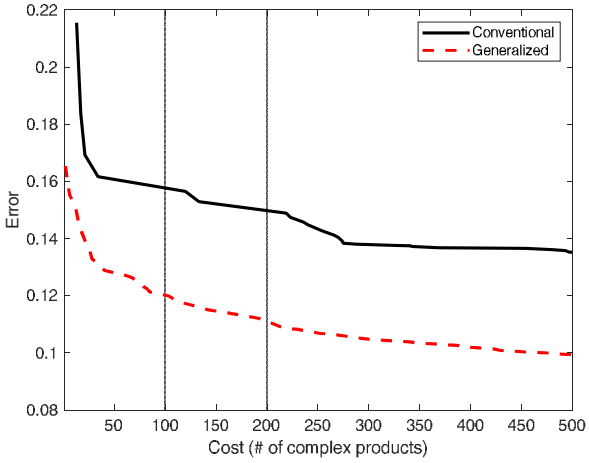

Fig. 13. Comparison of pruning for the two models in terms of setup costs: conventional (black) and generalized (red) models. For the same accuracy, the generalized model has much lower computational complexity, if the setup costs are also included. With a few tens of complex multiplications per sample, the generalized model has the same accuracy as the conventional model, requiring hundreds of complex multiplications.

E. Comparison with other LIP feedforward models

The generalized Volterra model with 9 coefficients, requiring 34 complex multiplications, achieves a residual EVM of 3% and shows no SER in the dataset. We use the static nonlinear model, the MP model [27], a trigonometric [33] and polynomial [34] FLANN model as a comparison.

Neural network models [35] typically involve multiple layered nonlinearities that make the models nonlinear in the parameter space, so that the LIP hypothesis is not fulfilled. An

exception are FLANN models with a linear output layer, including the random vector variant [36], but also radial basis function (RBF) models [37]. However, RBF models require a choice of the centers and width of the kernels which cannot be performed with linear estimation, whereas random vector functional link (RVFL) models have a random layer (chosen a priori) whose effectiveness depends on the choice of the random values. Hence, these models are out of scope for our comparison.

Restricted Volterra models are subsets of Volterra models, and thus their extension to complex-valued data is straightforward. For FLANN models, we consider the real and imaginary parts of the input and output signals as two separate channels, thus losing the structure of complex arithmetic. Hence, trigonometric FLANN models have 8 real coefficients for each delay m and order p, with basis functions $\cos(\pi p x[n-m])$ and $\sin(\pi p x[n-m])$. For polynomial FLANN models, terms are multiplied together alternating conjugated and non-conjugated complex terms to keep the terms around the carrier [38, 39].

As expected, static and restricted Volterra models are much less accurate, and though relatively simple, they are outperformed by pruned Volterra models. No such models achieve zero SER and EVM is larger. Static polynomials are no more effective than mere linear equalization. MP polynomials cause EVM to fall from 5.4% (equalization only) to 3.9%, at a cost of 26 parameters: hence, the models are more complex and less accurate. Trigonometric and polynomial FLANN models fare no better (EVM of 4.6 and 4.3%, respectively), with lower accuracy and larger complexity than the MP model. All these models have been tested with kernels up to the fifth order, and delays up to 4 terms.

The lower accuracy of these models is likely due to their relatively simple time structure, because there are no product terms derived from different input samples, unlike in Volterra models. The problem of complexity in Volterra models is thus better solved by extensive pruning than by a priori restrictions.

V. Conclusion

A novel model for nonlinear systems has been proposed and experimentally validated. The model is a generalization of complex Volterra models, and provides better accuracy and/or lower computational cost after pruning with the OMP and OBS methods. Hence, the model provides a significant improvement in the accuracy-complexity trade-off for the calibration of nonlinear systems.

The main idea is to perform calibration in the complex baseband domain with a model that is more general, more accurate, but more computationally expensive than the conventional Volterra model, and then prune the model to a much lower computational cost, though with the same accuracy as the pruned conventional Volterra model.

The fact that the generalized Volterra model is more general than the conventional one, as conventional Volterra models are a subset of the proposed class od models, implies that the model is more accurate, but also more complex. However, pruning is more effective in the generalized model than in the conventional Volterra model, and the computational complexity of the proposed model is significantly lower.

The computational cost advantage is due to two reasons: the number of free coefficients is lower for the same accuracy, and the setup cost is much lower. This is due to the fact that in the conventional Volterra model, a term of order 3 is computed as the time delayed, phase shifted and eventually frequency modulated sum of 4 different monomial terms, whereas in the generalized model there are 4 different coefficients, that are then pruned: hence, instead of computing four monomials of order 3, only one is needed. For 4th- and 5th- order kernels, the advantage is even more significant, as 8 and 16 monomials, respectively, are to be computed and summed together for every nonlinear coefficient, whereas the generalized Volterra model only uses one monomial.

The experimental results prove that the same accuracy (in terms of EVM) can be obtained with 9 coefficients in the generalized Volterra model, requiring the calculation of 34 complex products to compute all the basis functions. The conventional Volterra model requires 12 coefficients, but with a setup cost of 266 complex products. Hence, a 25% reduction in terms of number of coefficients to estimate, and an 87% reduction of setup costs, have been obtained. Such a large reduction in computational costs is mostly due to the fact that only one monomial term of degree p shall be computed for each coefficient of order p, instead of the sum of 2^{p-1} monomial terms of order p required in the conventional Volterra model for the same coefficient.

References

[1] B. Murmann, “Digitally assisted analog circuits,” *IEEE Micro*, vol. 26, no. 2, pp. 38-47, March-April 2006.

[2] M. Fayazi, Z. Colter, E. Afshari, R. Dreslinski, “Applications of artificial intelligence on the modeling and optimization for analog and mixed-signal circuits: A review,” *IEEE Trans. Circuits Systems I: Regular Papers,* vol. 68, no. 6, pp. 2418-2431, Mar. 2021.

[3] H. Le Duc, B. Feuvrie, M. Pastore and Y. Wang, “An adaptive cascaded ILA- and DLA-based digital predistorter for linearizing an RF power amplifier,” *IEEE Trans. Circuits Systems I: Regular Papers*, vol. 66, no. 3, pp. 1031-1041, Mar. 2019.

[4] J. Chani-Cahuana, P. N. Landin, C. Fager and T. Eriksson, “Iterative learning control for RF power amplifier linearization,” *IEEE Trans. Microw. Theory Techn.*, vol. 64, no. 9, pp. 2778-2789, Sep. 2016.

[5] L. Guan and A. Zhu, “Green communications: Digital predistortion for wideband RF power amplifiers,” *IEEE Microw. Mag.*, vol. 15, no. 7, pp. 84-99, Nov. 2014.

[6] M. Isaksson and D. Rönnow, “A parameter-reduced Volterra model for dynamic RF power amplifier modeling based on orthonormal basis functions,” *Int. J. RF Microw. Comput.-Aided Eng.*, vol. 17, no. 6, pp. 542-551, Nov. 2007.

[7] K. Dufrene, Z. Boos and R. Weigel, “Digital adaptive IIP2 calibration scheme for CMOS downconversion mixers,” *IEEE J. Solid-State Circuits*, vol. 43, no. 11, pp. 2434-2445, Nov. 2008.

[8] L. Anttila, M. Valkama and M. Renfors, “Frequency-selective I/Q mismatch calibration of wideband direct-conversion transmitters,” *IEEE Trans. Circuits Systems II: Express Briefs*, vol. 55, no. 4, pp. 359-363, Apr. 2008.

[9] F. Centurelli, P. Monsurrò, F. Rosato, D. Ruscio, and A. Trifiletti, “Calibrating sample and hold stages with pruned Volterra kernels,” *Electronics Letters*, vol. 51, no. 25, pp. 2094-2096, Dec. 2015.

[10] F. Centurelli, P. Monsurrò, F. Rosato, D. Ruscio, and A. Trifiletti, “Calibration of pipeline ADC with pruned Volterra kernels,” *Electronics Letters*, vol. 52, no. 16, pp. 1370-1371, Aug. 2016.

[11] S. Medawar, B. Murmann, P. Händel, N. Björsell, and M. Jansson, "Static integral nonlinearity modeling and calibration of measured and synthetic pipeline analog-to-digital converters," *IEEE Trans. Instrumentation and Measurement,* vol. 63, no. 3, pp. 502-511, Mar. 2014.
[12] P. Nikaeen and B. Murmann, "Digital compensation of dynamic acquisition errors at the front-end of high-performance A/D converters," *IEEE J. Selected Topics in Sig. Process.,* vol. 3, no. 3, pp. 499-508, June 2009.
[13] N. Björsell, P. Suchanek, P. Händel, and D. Rönnow, "Measuring Volterra kernels of analog-to-digital converters using a stepped three-tone scan," *IEEE Trans. Instrumentation and Measurement*, vol. 57, no.4, pp. 666-671, Apr. 2008.
[14] P. Monsurrò and A. Trifiletti, "Faster, stabler, and simpler - A Recursive-Least-Squares algorithm exploiting the Frisch-Waugh-Lovell theorem," *IEEE Trans. Circuits Systems II: Express Briefs*, vol. 64, no. 3, pp. 344-348, Mar. 2017.
[15] P. Monsurrò and A. Trifiletti, "Subsampling models of bandwidth mismatch for time-interleaved converter calibration," *IEEE Trans. Circuits Systems II: Express Briefs*, vol. 62, no. 10, pp. 957-961, Oct. 2015.
[16] P. Monsurrò, A. Trifiletti, L. Angrisani, and M. D'Arco, "Streamline calibration modelling for a comprehensive design of ATI-based digitizers," *Measurement: Journal of the International Measurement Confederation*, vol. 125, pp. 386-393, Sep. 2018.
[17] V. G. Mathews and G. L. Sicuranza, *Polynomial signal processing*. Wiley, USA, 2000.
[18] F. Centurelli, P. Monsurrò, G. Scotti, P. Tommasino, and A. Trifiletti, "Methods for model complexity reduction for the nonlinear calibration of amplifiers using Volterra kernels," *Electronics*, vol. 11, no. 19, 3067, Sep. 2022.
[19] G. Zhang, X. Hong, C. Fei, and X. Hong, "Sparsity-aware nonlinear equalization with greedy algorithms for LED-based visible light communication systems," *J. Lightwave Technology*, vol. 37, no. 20, pp. 5273-5281, July 2019.
[20] J.A. Becerra, M.J. Madero-Ayora, and C. Crespo-Cadenas, "Comparative analysis of greedy pursuits for the order reduction of wideband digital predistorters," *IEEE Trans. Microw. Theory Techn.*, vol. 67, no. 9, pp. 3575-3585, Sep. 2019.
[21] S. Haykin, *Neural networks and learning machines*, 3rd ed.; Pearson: Upper Saddle River, NJ, USA, 2009.
[22] B. Hassibi, D.G. Stork, and G.J. Wolff, "Optimal brain surgeon and general network pruning," Proc. 1993 IEEE Int. Conf. on Neural Networks, San Francisco, CA, USA, 28 March–1 April 1993, pp. 293–299.
[23] J.C. Patra, G. Panda, and R. Baliarsingh, "Artificial neural network-based nonlinearity estimation of pressure sensors," *IEEE Trans. Instrumentation and Measurement*, vol. 43, no. 6, pp. 874-881, Dec. 1994.
[24] M. Younes and F.M. Ghannouchi, "An accurate predistorter based on a feedforward Hammerstein structure," *IEEE Trans. Broadcasting,* vol. 58, no. 3, pp. 454-461, May 2012.
[25] J. G. Proakis and D. G. Manolakis, *Digital signal processing: Principles, algorithms and applications*. Upper Saddle River, NJ, USA: Prentice Hall, 1996.
[26] L. Hanzo, W. Webb, and T. Keller, *Single- and multi-carrier quadrature amplitude modulation*. Wiley, 2000.
[27] C. A. Schmidt, O. Lifschitz, J. E. Cousseau, J. L. Figueroa and P. Julián, "Methodology and measurement setup for analog-to-digital converter postcompensation," *IEEE Trans Instrumentation and Measurement*, vol. 63, no. 3, pp. 658-666, March 2014.
[28] D. R. Morgan, Z. Ma, J. Kim, M. G. Zierdt and J. Pastalan, "A generalized memory polynomial model for digital predistortion of RF power amplifiers," *IEEE Trans. on Signal Processing*, vol. 54, no. 10, pp. 3852-3860, Oct. 2006.
[29] Mini-Circuits, ZX60-100VH+ coaxial amplifier datasheet.
[30] Mini-Circuits, VAT-30+ attenuator datasheet.
[31] 4DSP, FMC150 user manual.
[32] Mini-Circuits, SLP-100 anti-aliasing lowpass filter datasheet.
[33] J. C. Patra, R. N. Pal, R. Baliarsingh, and G. Panda, "Nonlinear channel equalization for QAM signal constellation using artificial neural networks," *IEEE Trans. on Systems, Man, and Cybernetics, Part B (Cybernetics)*, vol. 29, no. 2, pp. 262-271, April 1999.
[34] J. C. Patra and A. C. Kot, "Nonlinear dynamic system identification using Chebyshev functional link artificial neural networks," *IEEE Trans. on Systems, Man, and Cybernetics, Part B (Cybernetics)*, vol. 32, no. 4, pp. 505-511, Aug. 2002.
[35] K. Burse, R. N. Yadav, and S. C. Shrivastava, "Channel equalization using neural networks: A review," *IEEE Trans. on Systems, Man, and Cybernetics, Part C (Applications and Reviews)*, vol. 40, no. 3, pp. 352-357, May 2010.
[36] B. Igelnik and Yoh-Han Pao, "Stochastic choice of basis functions in adaptive function approximation and the functional-link net," *IEEE Trans. on Neural Networks*, vol. 6, no. 6, pp. 1320-1329, Nov. 1995.
[37] D. Jianping, N. Sundararajan, and P. Saratchandran, "Communication channel equalization using complex-valued minimal radial basis function neural networks," *IEEE Transactions on Neural Networks*, vol. 13, no. 3, pp. 687-696, May 2002.
[38] M. Li, J. Liu, Y. Jiang, and W. Feng, "Complex-Chebyshev Functional Link Neural Network behavioral model for broadband wireless power amplifiers," *IEEE Trans. Microw. Theory Techn.*, vol. 60, no. 6, pp. 1979-1989, June 2012.
[39] G. T. Zhou, Hua Qian, Lei Ding, and R. Raich, "On the baseband representation of a bandpass nonlinearity," *IEEE Trans. on Signal Processing*, vol. 53, no. 8, pp. 2953-2957, Aug. 2005.

Cristian Bocciarelli was born in February 1998, in Narni (TR). He received the bachelor's and M.S. degrees (summa cum laude) in electronics engineering from the University of Rome La Sapienza, Italy, in 2019 and 2021, respectively. In November 2021 he started his PhD at the Department of Information Engineering, Electronics, and Telecommunications of University of Rome "La Sapienza". in electronic engineering. His research interests include the design and development of high speed ADC, wideband filters and digital calibration techniques of analog circuits. Furthermore, in the context of hardware security, his research activity is focused on side channel attacks on cryptography primitive.

Francesco Centurelli was born in Roma in 1971. He received the laurea degree (cum laude) and the Ph.D. degree in Electronic Engineering from the University of Roma "La Sapienza", Roma, Italy, in 1995 and 2000 respectively.
In 2006 he became an Assistant Professor at the DIET department of the University of Roma La Sapienza.
His research interests were initially focused on system-level analysis and design of clock recovery circuits and high-speed analog integrated circuits, and now concern the design of analog-to-digital converters and very low-voltage circuits for analog and RF applications.
He has published more than 100 papers on international journals and refereed conferences, and has been also involved in R&D activities held in collaboration between Università "La Sapienza" and some industrial partners.

Pietro Monsurrò was born in Rome, Italy. He received the Ph.D. degree in electronic engineering from the Department of Electronic Engineering, University of Rome "La Sapienza" Italy, in 2008. He is currently Assistant Professor at the Department of Information Engineering, Electronics and Telecommunications of the University of Rome "Sapienza", Italy.
His current research interests include low-voltage low-power analog and mixed-signal circuits in advanced CMOS processes, analog filter design in CMOS and BiCMOS processes, behavioral models of mixed-signal and RF systems, digital background calibration techniques for pipeline and time-interleaved analog to digital converters, advanced time-interleaved architectures, model identification, and adaptive algorithms.

Giuseppe Scotti received the M.S. and Ph.D. degrees in electronic engineering from the University of Rome “La Sapienza”, Italy, in 1999 and 2003, respectively. In 2010, he became a Researcher (Assistant Professor) at the DIET department of the university of Rome "La Sapienza" and in 2015 he was appointed Associate Professor in the same department. His research activity was mainly concerned with integrated circuits design and focused on design methodologies able to guarantee robustness with respect to parameter variations in both analog circuits and digital VLSI circuits. In the context of analog design his research activity was concerned with circuit topologies for the realization of low-voltage analog building blocks using ultra-short channel CMOS technology, whereas in the context of cryptographic hardware his focus has been on novel PAAs methodologies and countermeasures. He has been also involved in R&D activities held in collaboration between “La Sapienza” University and some industrial partners, which led, between 2000 and 2015, to the implementation of 13 ASICs. He has coauthored more than 70 publications in international Journals, about 70 contributions in conference proceedings and is the co-inventor of 2 international patents.

Valerio Spinogatti was born in Rome (Italy) in 1997. He received the Master Degree in Electronic engineering from University of Rome “La Sapienza”, Rome, Italy, in 2021. He’s currently a PhD student at the Department of Information Engineering, Electronics, and Telecommunications of University of Rome “La Sapienza”.
His research interests include high-speed analog-to-digital converters, digital calibration techniques based on adaptive filters for communication systems and fast digitizers, and analog wideband filters. He is also working in the field of hardware security, where he is focusing on side channel attacks on implementations of cryptographic primitives.

Pasquale Tommasino received the Master degree in Electronic Engineering and the Ph. D. degree from the University of Rome "La Sapienza" in 1992 and 1999 respectively.
Since 1995, he has been with the Electronic Engineering Department (now Department of Information Engineering, Electronics and Telecommunications) of the University of Rome "La Sapienza", where from 2007 he is Assistant Professor. His research interests are mainly oriented to the design of RF and microwave broadband circuits. Presently, he is mainly engaged in the design of integrated circuits for E-band transceivers.

Alessandro Trifiletti was born in Rome (Italy) on October 4, 1959. In 1991 he joined Electronic Engineering Department of “La Sapienza” University in Rome as research assistant, where he was involved in research activities dealing with analogue, RF and microwave IC’s design. In 2001 he became assistant professor and in 2005 he got the position of associate professor and in 2019 the position of Full Professor at the Engineering Faculty of the same University. Prof. Trifiletti has worked in the field of Microelectronics, both from the point of view of design methodologies and circuit topologies. On these subjects, Prof. Trifiletti has (co-)authored over 210 publications, of which about 80 published on international Journals, the others published on the proceedings of major international Conferences (a large part of these sponsored by the IEEE). He is presently reviewer for some IEE and IEEE reviews, among them: IEEE Transaction on Microwave Theory and Techniques, IEEE Transaction on Circuit and Systems (part I and II), IEE Proceedings on Circuits, Devices and Systems, IEE Electronic letters. In last 20 years he has been engaged in the coordination of research teams from DIET (previously DIE) in the framework of national and international programs, involving both industrial and academic partners. From an industrial perspective, Prof. Trifiletti expertise covers topics about analogue and RF microelectronics, Radar and ESM systems, high-speed communication systems, security issues in cryptographic algorithms implementation, and embedded system design.